Modeling and experimental verification of common dielectrophoresis on platinum microelectrodes

Flavio Humberto Fernández Morales
Universidad Pedagógica Y Tecnologica de Colômbia
Carrera 18 Calle 22, Duitama, Boyacá, Colômbia.
flaviofm@telecom.com.co

Julio Enrique Duarte
Universidad Pedagógica Y Tecnológica de Colômbia
Carrera 18 Calle 22, Duitama, Boyacá, Colômbia.
julioenriqueduarte@latinmail.com

Joseph Samitier Martí
Universitat de Barcelona
08028, Barcelona, Espanha
smairtier@el.ub.es

(Recebido: 24 de agosto de 2005)

Abstract: The motion of neutral matter induced by non-uniform electric fields, i.e. common dielectrophoresis, has become the basic phenomenon of microchips intended for medical, biological and chemical assays, especially when they imply biological and artificial microparticle manipulation. This paper describes the modeling and experimental verification of an interdigitated castellated microelectrode array intended to handle biological objects, based on the dielectrophoretic effects. The proposed design, a whole microsystem including electrical, optical and fluidic interfaces, was developed employing platinum deposited by lift-off, silicon micromachining, and photoresin patterning techniques. The fabricated electrodes have typical dimensions of 50, 70 and 90 μm, and were tested by means of polystyrene microspheres of 4.2 μm in diameter. Positive and negative dielectrophoresis were clearly observed, and the microparticle behavior was coherent with that predicted by the homogeneous particle model as well as with the electric field distributions assessed by the finite element method. The most relevant results are reported here.

Key-words: dielectrophoresis, microparticle manipulation, microsystems

1 Introduction

Common dielectrophoresis (c-DEP) has become the basic phenomenon of microchips intended for medical, biological and chemical assays, especially when they imply biological and artificial microparticle manipulation [1,2]. Furthermore, c-DEP has been employed as an additional mechanism to develop new materials which require the location of micro and nanoparticles in a precise manner on surfaces with the desired shapes [3,4].

The importance of c-DEP remains on the simple way that it can be generated because it only requires a few electrodes of size similar to that of particles to be handled. Thus, microsystems have gained a huge preponderance as a technology that suits very well the requirements of miniaturized microstructures aimed to handle biological objects in order to obtain more confident, faster and cheaper biochemical assays [5]. Diverse materials and technological approaches have been suggested to fabricate these microtools, but silicon substrates with electrodes made in noble metals are usually employed to manufacture such devices [6,7].

This paper deals with the modeling and experimental verification of a shifted castellated microelectrode array intended to handle biological objects, based on the dielectrophoretic effects. The proposed design, a whole microsystem including electrical, optical and fluidic interfaces, was developed employing platinum electrodes deposited by lift-off, silicon micromachining, and photoresin patterning techniques. The fabricated electrodes have typical dimensions of 50, 70 and 90 μm, and were tested by means of polystyrene microspheres of 4.2 μm in diameter. Positive and negative dielectrophoresis were clearly observed, and the microparticle behavior was coherent with that predicted by the homogeneous particle model as well as with the electric field distributions assessed by the finite element method. The most relevant results are reported here.

2 Methods and Materials

2.1 Common dielectrophoresis

When an uncharged body is placed in a non-uniform electric field, it induces electrical charges upon the particle surface. This charge distribution will have equal quantities of positive and negative electric charges, and can be modeled as an equivalent dipole. The electric field will cause an alignment action on the dipoles with regard to itself. As the field is non-uniform, one dipole end will be in a weaker region than the other, which will originate a net force acting on the induced dipoles and cause them to be constrained to move towards or away from the region of highest field density. This motion is termed dielectrophoresis (DEP) and it stands for the so-called conventional or common dielectrophoretic (c-DEP) phenomena [8].

For a non-ideal insulating spherical particle of radius r suspended in a medium of relative effective permittivity ε_m and interacting with a non-uniform electric field of strength E, the time-averaged dielectrophoretic force is given by [9]:

$$\mathbf{F_{DEP}} = 2\pi\varepsilon_0\varepsilon_m r^3 \mathrm{Re}[\mathrm{F_{CM}}]\nabla|\mathbf{E}|^2 \quad (1)$$

Where ε_0 = 8.854x10-12 (Farad m-1) is the free-space permittivity, ∇ is the gradient operator and Re[FCM] denotes the real part of the polarizability function, so called the Clausius-Mossotti factor, defined by [10]:

$$F_{CM} = \frac{\left(\varepsilon_p^* - \varepsilon_m^*\right)}{\left(\varepsilon_p^* + 2\varepsilon_m^*\right)}, \quad (2)$$

where p and m stand for particle and medium, respectively. The relative complex dielectric permittivity is given by:

$$\varepsilon^* = \varepsilon_0\varepsilon - j\,\sigma/\omega, \quad (3)$$

where ω is the relative effective permittivity, σ is the effective conductivity, ω is the angular frequency of the applied field and the symbol $j = \sqrt{-1}$ signifies that the dielectric displacement current leads the conduction current by a phase angle of 90°.

From equation (1) it can be seen that FDEP depends on the particle size, as well as on the magnitude of the electric field which is related to the electric potential applied. The gradient operator represents the spatial non-uniformity of the electric field, which is a geometrical factor depending on the electrode layout. In fact, the non-uniformity factor (∇ E2) varies as the square of the applied voltage multiplied by a factor characteristic of the electrode geometry [11]. Furthermore, FDEP can actuate on both direct current (DC) and alternating current (AC) fields as a consequence of its sign independence of the electric field polarity, justified by the proportionality of the force to the square of the electric field magnitude. In addition, the direction of this dielectrophoretic force depends on the polarity of the induced dipole moment, which in turn is determined by the conductivities and permittivities of the particle and its suspending medium, i.e. the particle motion direction depends on the Clausius-Mossotti factor polarity.

The right particle model selection depends on the particle characteristics itself as: geometry, shape and internal structure. Thus, for a polystyrene microbead the homogeneous sphere model can be used. However, when behavior of biological cells such as viruses, bacteria or protoplasts must be explained, the single-shell or multishell models can be employed [12, 13]. In this case it was selected the homogeneous particle model represented by equation (2).

When conduction and polarization mechanisms are considered simultaneously, the effective polarizability of real dielectrics becomes a complex function relating

both conductivity and permittivity as can be seen in equation (2). Plotting both real and imaginary parts of the polarizability function is one of the most useful techniques to predict the behavior of particles in non-uniform electric fields with respect to changes in the electric field frequency, as well as in the electrical properties of particles and medium [14].

In order to illustrate such parametric dependencies, the real ($Re[F_{CM}]$) and imaginary ($Im[F_{CM}]$) parts of the F_{CM} for a latex sphere submersed in water are depicted in figure 1. Of course, the appearance of F_{CM} hinges upon the particle model selected.

Figure 1 shows the existence of a single relaxation frequency in the particle-medium system, as predicted by the homogeneous particle model. The relaxation is represented by either the sign change of the real part of the function or the negative peak in its imaginary part.

Figure 1. Magnitude of: (a) Re[FCM] and (b) Im[FCM] versus frequency for δm varying between 0 and 1 S m^{-1}. The parameters used are $\varepsilon p = 3.5$, $\varepsilon m = 80$ and $\delta p =$ 9 mS m^{-1}. In a real experimental situation δm remains the main parameter that is completely at the experimentalist's disposal

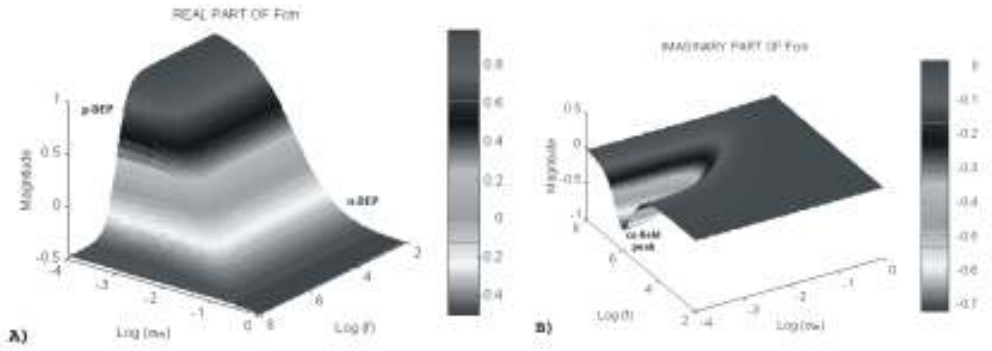

As depicted in figure 2, c-DEP can be divided into two phenomena. The first one is known as positive dielectrophoresis (p-DEP). It is characterized by the particle motion towards the strongest, or maximum, region of the electric field as a consequence of a positive value of the Re[FCM]. p-DEP occurs for particles that are more polarizable than the medium, i.e. when the effective permittivity and/or conductivity of the particle are higher than that of its surrounding medium. On the other hand, if the particle polarizability is low enough for the Re[FCM] to become negative, the FDEP will tend to move the particle towards the weakest, or minimum, region of the electric field. This phenomenon is called negative dielectrophoresis (n-DEP).

Figure 2. The principle of DEP represented by two different particles in a non-uniform electric field. The particle on the left is more polarizable than the surrounding medium and is attracted towards the strong field at the pin electrode (p-DEP), whilst the particle of low polarizability on the right is directed away from the strong field region (n-DEP) [15]

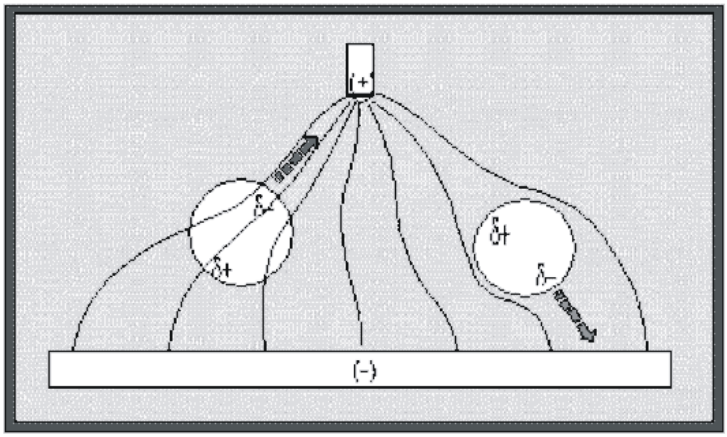

2.2 Modeling and simulation of the electric field

Modeling DEP phenomena may be addressed in two ways. The first one involves modeling the particle polarizability function. The second way entails the careful calculation of the electric field distribution over the electrodes, as this distribution determines the non-uniformity geometrical factor that in the case of c-DEP establishes where particles are collected or rejected. In other words, when aware of the location of the maximum and minimum of the electric field, one can predict whether particles will be attracted to or repelled from a region, based on the polarizability function sign.

In view of the critical role played by field inhomogeneities, the field distribution over the electrode arrays must be assessed. Calculations presented in this section were carried out by means of the commercial program ANSYS (Swanson Analysis Systems, Inc.), which is a general purpose software that uses the Finite Element Method (FEM) to solve physical problems [16] It can be stressed that, taking advantage of symmetries, 2-D models usually suffice to assess the electrode operation in dielectrophoretic applications. However, when the possible particle spatial distributions have to be predicted, utilizing 3-D models becomes mandatory.

Periodical arrays of interdigitated castellated electrodes are one of the most popular electrode designs when particle collection or spatial separation at well-established locations are required [17]. As depicted in figure 3(a), shifted interdigitated castellated microelectrode approach is that in which tips of electrodes of one polarity face bays of electrodes of the other polarity, and vice versa. The FEM

model is also shown in figure 3(b), within which lighter areas represent the electrode surfaces where the driving voltage is applied.

Figure 3. (a) Shifted interdigitated castellated microelectrode pattern. (b) 3-D mesh of the shifted interdigitated castellated electrodes. The castellation size and medium height is 50 μm

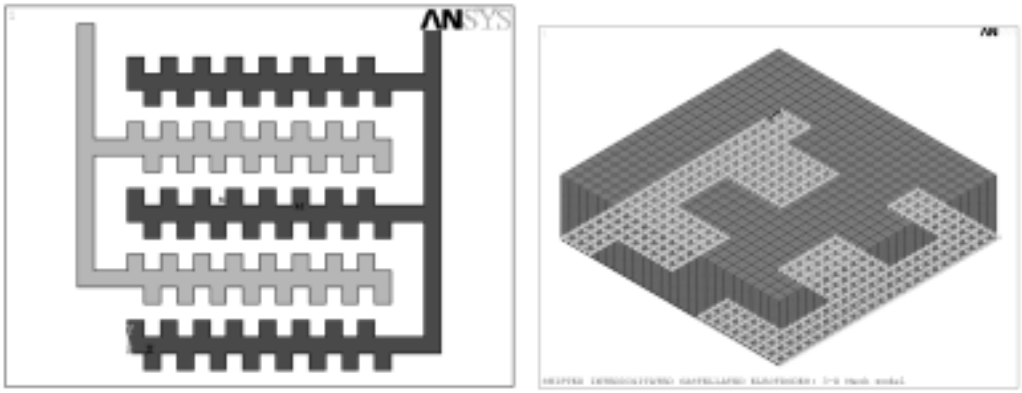

As a result of the electric potential distribution, the electric field spatial distribution takes its maximum values at points located near the corners of the electrode castellation tips (see figure 4).

Figure 4. Pseudo-topographic representation of the electric field, in V μm^{-1}, plotted on a plane located 2 μm over the electrode surface. The voltage applied was ±5 V

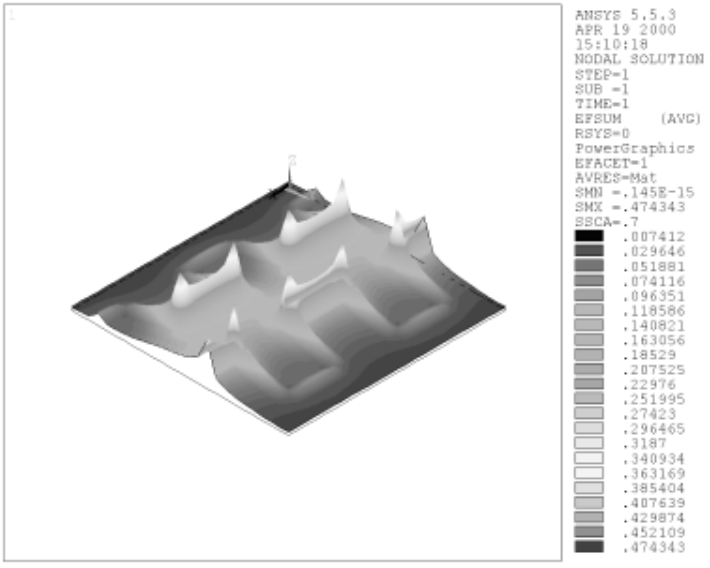

For the sake of simplicity, only a plane located at 2 μm over the electrode surface is analyzed. It can be seen that points located near to the electrode tips will experience the highest electric field strength, whilst this strength diminishes as the observation point moves towards the central part of the interelectrodic gap, towards the bays or onto the metallic surface of the electrodes.

The computer analysis predicts that p-DEP will result in the agglomeration of particles at electrode tips, while n-DEP will cause particles to accumulate on electrode bays and on the electrode surface, as well as in the interelectrodic gap. Of course, the final particle position depends upon the polarizability function value.

One of the most amazing possibilities envisaged for the castellated microelectrodes is that multiple-particle mixtures (two or even more particle types) could be physically separated into different regions, on the basis of their electrical properties. Besides this, an additional force can be used to drag away the desired fraction of particles, collecting them for further assays. However, one must be aware that such a separation involves a careful choice of the experimental conditions, especially the suspending medium conductivity.

2.3 Microsystem description

The proposed design is a whole microsystem including electrical, optical and fluidic interfaces. The technological process at the wafer level can be roughly divided into three stages. The first one is the microelectrode patterning in which metal electrodes are defined onto a silicon wafer of 300 μm thickness by lift-off to pattern platinum electrodes. After that, the wafer is drilled by bulk silicon micromachining in order to shape the inlet and outlet holes. The wafer-level processing ends up with the photolithographic structuring of an UV-curable polymer to cast the microchamber walls. The microchip processing was carried out at the Microelectronics National Center in Barcelona, Spain.

As a result of the fabrication process it was obtained a microchip 8291 μm in width and 11200 μm in length, giving a total area of 92.86 mm2. The electrode microstructure tested in this work is actually composed by three microarrays (see figure 5), each one formed by classical and shifted interdigitated castellated electrodes, as well as saw-teeth electrodes with typical sizes of 50, 70 and 90 μm in both electrode length and separation. In order to gain flexibility, electrodes of different size have their own pads for external connection.

Figure 5. Partial view of the microsystem containing classical and shifted interdigitated castellated, as well as saw-teeth microelectrodes. Micropool walls and a micromachined hole can also be observed.

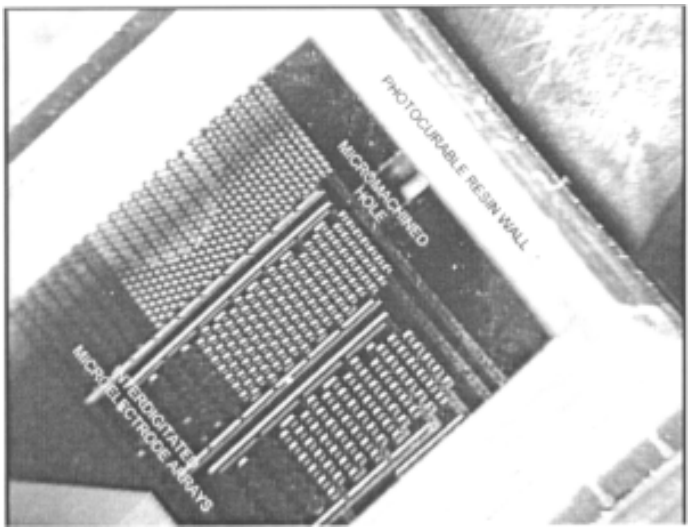

2.4 Experimental set-up

As it can be seen in figure 6, the instrumentation required to perform particle microhandling can be roughly separated into three parts. The first one is the electronic subsystem that includes: signal generator, amplifier, oscilloscope, and impedance analyzer. The power signal was supplied by a Hewlett Packard 33120 A function generator and the electrical signal calibration was allowed by means of a Tektronix TSD 220, 100 MHz, two channel digital real-time oscilloscope. Furthermore, an impedance analyzer could be used to check the structure's impedance in order to provide an alternative read out system, getting round the optical approach.

Figure 6. Block diagram of the most relevant apparatus required to perform the practical work and the relationship among them. Dotted lines indicate those instruments which do not have to be continuously attached during the experiment

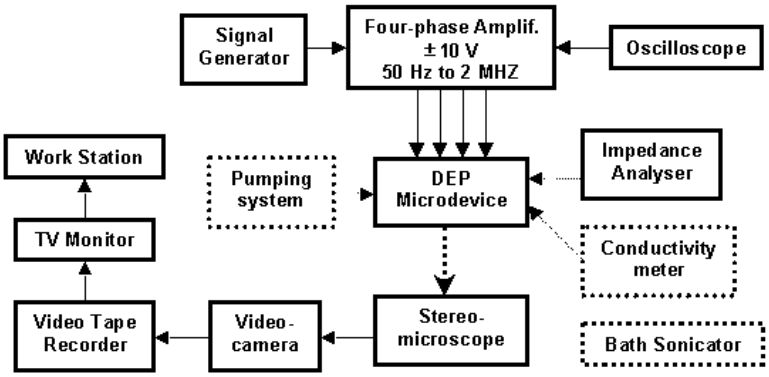

The second subsystem is the particle microhandler itself, which contains the microelectrodes under study. The third part is the optical subsystem that is able to observing and recording the electrokinetic particle behavior. The experimental work was performed employing a stereomicroscope Karl Zeiss SV 11 with a Sony CCD video color camera SSC-370 P, as well as a videotape recorder attached to it. Moreover, there was a color video monitor, Sony KX-1410 QM, connected in parallel to supervise the experiments. Furthermore, taking advantage of a PC provided with a professional quality PCI motion-JPEG card, Aver Media® MV-300, the particle motion behavior could be analyzed digitizing the captured video images and making a frame-by-frame study of them. This subsystem is complemented by a cold-light source, which allows light filtering and polarization.

Figure 6 also shows other apparatus which are also required to carry out the experimental work. Thus, the bath sonicator is an ultrasound generator valuable to maintain microparticles in their monodisperse state. The liquid medium conductivity was measured by means of a Corning® 441 conductivity meter.

2.5 Microparticles and medium

Before using biological samples, the device operation can be analyzed using polystyrene microspheres. These particles are frequently employed in laboratory assays and diagnosis to detect different types of antibodies [18]. Additionally, latex microbeads have physical properties (size and density) quite similar to those of biological cells. In view of their manifold applications and because of controlling concentration and preparing suspensions of latex microparticles is easier than doing it with bioparticles, such latex microspheres have become the most popular instruments to test microstructures intended for DEP applications.

In this work polystyrene microspheres of 4.2 μm in diameter (5% of solids in water, supplied by Molecular Probes Inc., Eugene, Oregon, USA) were available to experiment on the proposed microdevice. Accordingly to the microbeads' manufacturer instructions, microparticles were diluted in de-ionized water, $\delta m = 2x10^{-4}$ S m^{-1} at 28°C, in a ratio of 1 to 200 with respect to the original concentration. The typical sample volume was 100 μL.

The suspending medium was micropipetted onto the electrode active area by means of an Eppendorf® micropipette dispenser with variable volume between 10 and 100 μL. Before the liquid was used the application of ultrasound between 3 and 5 minutes was routinely done. Once the solution had been dropped onto the chip and before the driving voltage was turned on, a waiting time of around 30 seconds was respected to allow the sample stabilization while particles lost the kinetic energy gained during the fall.

3 Results and Discussion

3.1 Positive and negative DEP

Having dropped the particle dissolution into the micropool, electrodes of 70 μm were energized with a sinusoidal signal of 7 V in amplitude and 10 MHz. After a few minutes, particles were concentrated forming clusters located at the electrode bay regions of shifted interdigitated castellated arrays, i.e. particles were driven towards and agglomerated at regions corresponding to the electric field minima, as predicted by simulations of the electric field described in section 2.2. The aforementioned behavior, i.e. particles of 4.2 μm in diameter affected by n-DEP, was observed till a frequency of approximately 1.2 MHz as illustrated in figure 7.

Figure 7. Zoomed view of shifted castellated microelectrodes of 70 μm in typical dimension. Clusters of polystyrene microbeads (lighter clouds) of 4.2 μm in diameter diluted in de-ionized water (δ_m = 2 μS cm^{-1}) in a ratio of 1 to 200, can be seen at the bay regions affected by n-DEP. A sinusoidal signal of 7 V in amplitude and 1.3 MHz in frequency was applied

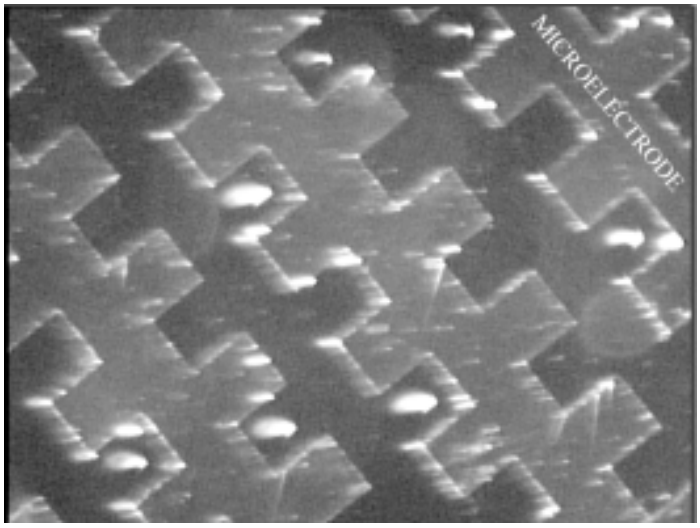

When the frequency of the applied signal is decreased, maintaining unaltered the voltage amplitude, particle motion towards the electrode corners is observed. In other words, the particle clusters previously described are now attracted towards the highest electric field regions, verifying the p-DEP phenomenon on the microelectrode array of 70 μm. This behavior is evident for instance at 200 kHz. Interestingly, particles remain attached to the electrode corners till the frequency is risen again to a value in which n-DEP can stably occur, i.e. if frequency is increased, particles are repelled towards their original positions at the electrode bays. In other words, the occurrence of n-DEP and p-DEP can be successively achieved by simply changing and selecting the right values for the applied frequency signal. Figure 8, in which the observation area is the same as in figure 7, proves the occurrence of p-DEP in a microelectrode array of 70 μm where particles are attached to the corners of shifted microstructures.

Figure 8. Zoomed view of shifted castellated microelectrodes of 70 μm in typical dimension. Clusters of polystyrene microbeads (lighter clouds) of 4.2 μm in diameter diluted in de-ionized water (δ_m = 2 μS cm^{-1}) in a ratio of 1 to 200, can be seen at the electrode corners affected by p-DEP. A sinusoidal signal of 7 V in amplitude and 100 kHz in frequency was applied

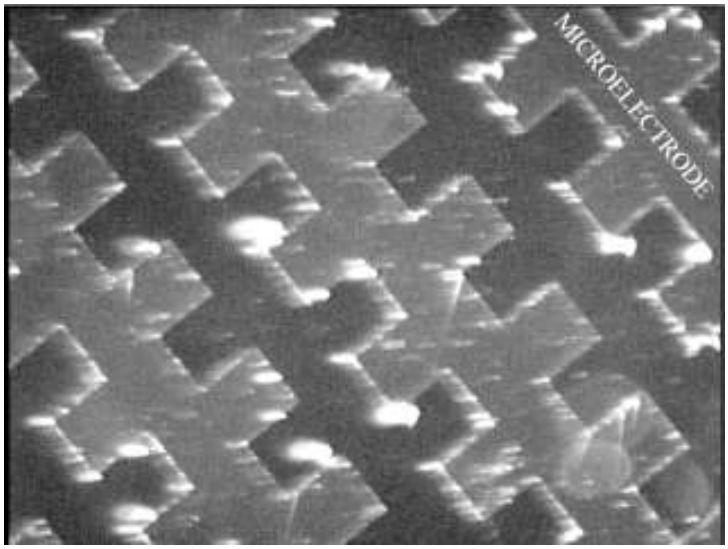

3.2 Influence of the applied frequency

As previously described, frequency variations produce particle motion towards well-defined regions on the microelectrode array. In our experiments frequencies above around 1.2 MHz compel particles to concentrate at the electric field minima, i.e. n-DEP is induced onto them. On the other hand, lower frequencies were observed to produce particle attraction towards the electrode edges where the electric field strength is maximum, i.e. p-DEP has occurred.

These results can be explained according to the homogeneous particle model. For the experimental values δ_m = 2x10^{-4} S m^{-1} and ε_m = 80, taking the particle permittivity ε_p = 3.5 [19], and considering its conductivity δ_p = 6.2 mS^{-1} as the best fitting of the Clausius-Mossotti factor, the crossover frequency, fc, is 1 MHz (see figure 9). It means that for frequencies above fc, particles will experience n-DEP while for frequencies below fc, the opposite is true.

Figure 9. Real part of the Clausius-Mossotti factor for a polystyrene microsphere. The crossover frequency, *fc*, is 1 MHz

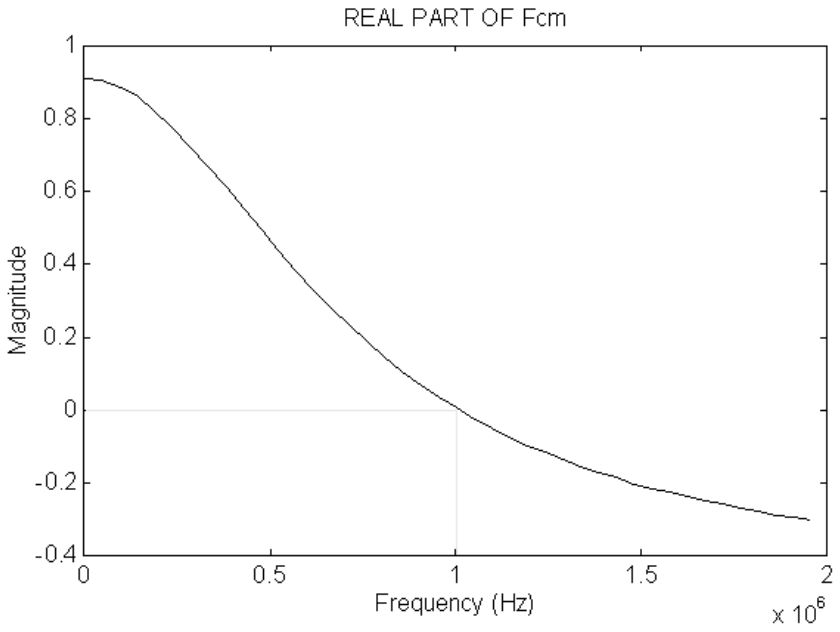

In view of the experimental results one can say that the occurrence of c-DEP in polystyrene microbeads was successfully experimentally verified. Since the point of view of frequency changes, the homogeneous particle model and its related Clausius-Mossotti factor explains coherently the observed particle behavior. In other words, particle behavior is consistent with that described by the particle model corresponding to a homogeneous sphere.

3. 3 Influence of the electrode size

Figure 10 shows the occurrence of n-DEP with the same particle concentration than that of the preceding photographs, verified in the microelectrode array of 50 μm.

Figure 10. Clusters of polystyrene microbeads of 4.2 μm in diameter diluted in de-ionized water (δ_m = 2 μS cm^{-1}) in a ratio of 1 to 200, affected by n-DEP. A sinusoidal signal of 5 V amplitude and 1.5 MHz in frequency was applied. Particle clusters (bright points) can be seen concentrated at the bay regions of a shifted interdigitated castellated microelectrode.

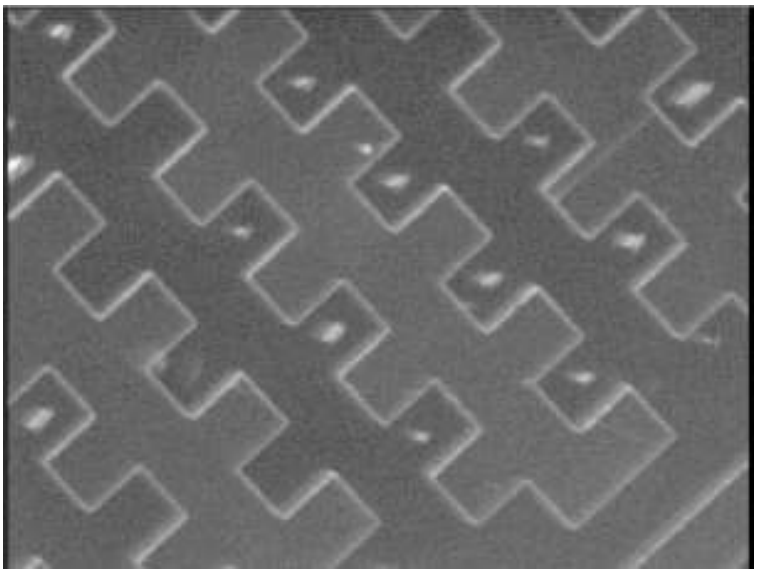

It must be pointed out that size reduction of the typical microelectrode dimensions (50 μm in figure 10) results in a lower voltage required to bring about the dielectrophoretic phenomena. Furthermore, such a behavior does not alter the particle distribution over the electrode surface. This is illustrated in figure 10 where microelectrodes are driven by a signal of 5 V compared to 7 V in the case of microelectrodes of 70 μm, or even 10 V in microstructures of 90 μm in typical electrode size. In these cases, the maximum electric field intensity is 1 V μm^{-1}. In fact, one of the main advantages of scaling down the electrode dimensions is that the same field strength may be produced utilizing smaller voltages, which will be valuable when working with biological cells in order to reduce the possibility of physical damages caused by high voltages.

In view of the preceding results one can say that the occurrence of c-DEP was not affected by reducing the typical dimensions, castellation size and electrode separation, of the studied structure. As the microelectrode size is reduced, the required voltages also go down, maintaining stable the particle distribution which is consistent with the electric field profile over such electrode geometries.

4 Conclusions

This work was conceived to explore the possibilities of microsystems aimed at bioparticle handling based on the different dielectrophoretic effects. To attain this goal, activities were orientated towards the design, fabrication and testing of microstructures which adapt themselves to the electrohandling of both artificial and natural microparticles.

In order to achieve a good understanding of the related phenomena, modeling tasks begin with a description of the electrical model, which includes the particle modeling and the electrical field calculations. It is worth mentioning that the 3-D approach gives a bit more insight into the electric field shapes than that gained with 2-D models. However, the use of the former rather than the latter will depend on the designer's needs.

From a technological point of view, a whole microsystem was designed and fabricated by means of microfabrication techniques. Such a microstructure includes a silicon substrate onto which electrodes of platinum were grown by lift-off technique to fulfill biocompatibility requirements. Moreover, the substrate was drilled to shape the inlet and outlet fluid ports employing bulk silicon micromachining. Microcavity walls were molded by means of a photopatternable resin. As a result of this process, a micropool of known volume is formed allowing the use of the same sample volume during all the experimental stages.

From the experimental point of view, microstructures were tested with polystyrene microspheres of 4.2 μm in diameter. Thus, positive and negative dielectrophoresis has been successfully experimentally verified with polystyrene microbeads, as well as the influence of variations in the electrical signal applied, and the effects of the electrode size on the particle behavior. Furthermore, the particle behavior observed has been evaluated and is consistent with the results based on the particle model corresponding to a homogeneous sphere, which explains n-DEP and p-DEP observations in terms of the crossover frequency.

Besides the particle model which explain the frequency dependencies of the particle behavior, numerical calculations of electric field were also validated, because artificial particles, under the influence of n- or p-DEP, were observed to collect over the microelectrodes, according to distributions dictated by the electric field shape.

To conclude, it can be said that dielectrophoresis as a subject of research in general, and microsystems aimed at bioparticle microhandling hinging upon dielectrophoretic phenomena in particular, have a brilliant future. Some reasons for this are that microsystems can be manufactured with dimensions adequate for those required by microparticle manipulation, and the dielectrophoretic force has magnitudes comparable to those of the other forces available to perform these tasks. Furthermore, the method is non-invasive, does not require the use of antibodies or other labeling and can be employed at either the single-cell or multiple-cell level.

5 References

[1] Müller, T., Pfennig, A., Klein, P., Gradl, G., Jäger, M., Schnelle, T. (2003). The potential of dielectrophoresis for single-cell experiments. IEEE, *Medicine and Biology Magazine*, v. 22, p. 51 - 61.

[2] Hoettges, K., Hughes, M., Cotton, A., Hopkins, N., McDonell, M. (2003). Optimizing particle collection for enhanced surface-based biosensors. IEEE in *Medicine and Biology Magazine*, v. 22, p. 68 - 74.

[3] Velev, O., Kaler, E. (1999). In *situ assembly* of colloidal particles into miniaturized biosensors. Langmuir, v. 15, p. 3693 – 3698.

[4] Rosenthel, A., Voldman, J. (2005). Dielectrophoretic traps for single-particle patterning. *Biophysical Journal*, v. 88, p. 2193 - 2205.

[5] Fuhr, G., Shirley, S. G. (1998). Biological application of microstructures. *Topics in Current Chemistry*, v. 194, p. 83 - 116.

[6] Pethig, R., Burt, J. P. H., Parton, A., Rizvi, N., Talary, M. S., Tame, J. A. (1998). Development of biofactory-on-a-chip technology using excimer laser micromachining. Journal *of Micromechanics and Microengineering*, v. 14, p. 57 - 63.

[7] Schnelle, T., Müller, T., Voigt, A., Reimer, K., Wagner, B., Fuhr, G. (1996a). *Adhesion-Inhibited surfaces*. Coated and uncoated interdigitated electrode arrays in the micrometer and submicrometer range. Langmuir, v. 12, p. 801 - 809.

[8] Pohl, H. A. (1951). The motion and precipitation of suspendoids in divergent electric fields. *Journal of Applied Physics*, v. 22, p. 869 - 871.

[9] Pohl, H. A., Pethig, R. (1977). Dielectric measurements using non-uniform electric field (dielectrophoretic) effects. *Journal of Physsics E: Scientific Instruments*, v. 10, p. 190 - 193. Corrigendum p. 883.

[10] Brown, A. P. (1996). *Dielectrophoretic investigations of bacterial cells*. PhD. Dissertation, University of York, York, United Kingdom.

[11] Feeley, C. M., Pohl, H. A. (1981). The influence of resistivity and permittivity on the motion of uncharged solid particles in non-uniform electric fields (the 'dielectrophoretic effect'). *Journal of Physics D: Applied Physics*, v. 14, p. 2129 - 2138.

[12] Gascoyne, P. R. C., Becker, F. F., Wang, X-B. (1995). Numerical analysis of the influence of experimental conditions on the accuracy of dielectric parameters derived from electrorotation measurements. *Bioelectrochemistry and Bioenergetics*, v. 36, p. 115 – 125.

[13] Kakutani, T., Shibatani, S., Sugai, M. (1993). Electrorotation of non-spherical cells: theory for ellipsoidal cells with an arbitrary number of shells. *Bioelectrochemistry and Bioenergetic*s, v. 31, p. 131 – 145.

[14] Fuhr, G., Müller, T., Schnelle, T., Hagedorn, R., Voigt, A., Fiedler, S. (1994). Radio-frequency microtools for particle and living cell manipulation. *Naturwissenschaften*, v. 81, p. 528 - 535.

[15] Stephens, M., Talary, M., Pethig, R., Burnett, A., Mills, K. (1996). The dielectrophoresis enrichment of CD34+ cells from peripheral blood stem cell harvests. *Bone Marrow Transplantation*, v. 18, p. 777 - 782.

[16] Kohnke, P. (1995). *ANSYS Theory Reference Manual release 5.5. Swanson Analysis Systems Inc.*

[17] Gascoyne, P. R. C., Huang, Y., Pethig, R., Vykoukal, J., Becker, F. F. (1992). Dielectrophoretic separation of mammalian cells studied by computarized image analysis. *Measurement Science and Technology*, v. 3, p. 439 - 445.

[18] Coakley, W. T. (1997). Ultrasonic separations in analytical biotechnology. *Trends in Biotechnology*, v. 15, p. 506 - 511.

[19] Müller, T., Gradl, G., Howitz, S., Shirley, S., Schnelle, T., Fuhr, G. (1999). A 3-D microelec*trode system for handling and caging single cells.* Biosensors and Bioelectronics, v. 14, p. 247 – 256.